


 Cite this: *RSC Adv.*, 2023, **13**, 14217

# Reversible adsorption of iridium in lyophilized cells of the unicellular red alga *Galdieria sulphuraria*†

 Ayumi Minoda,<sup>a</sup> Shuya Ueda,<sup>b</sup> Shin-ichi Miyashita,<sup>c</sup> Toshihiko Ogura,<sup>d</sup> Sachika Natori,<sup>e</sup> Jing Sun<sup>e</sup> and Yoshio Takahashi<sup>e</sup>

Iridium (Ir) is one of the rarest elements in the Earth's crust and is valuable in industry due to its high corrosion resistance. In this study, we used lyophilized cells of a unicellular red alga, *Galdieria sulphuraria* for the selective recovery of small amounts of Ir from hydrochloric acid (HCl) solutions. The Ir recovery efficiency of the lyophilized cells was higher than that of activated carbon and comparable to that of an ion-exchange resin in up to 0.2 M acid. Lyophilized *G. sulphuraria* cells showed different selectivity from the ion-exchange resin, adsorbing Ir and Fe in 0.2 M HCl solution while the ion-exchange resin adsorbed Ir and Cd. The adsorbed Ir could be eluted with more than 90% efficiency using HCl, ethylenediaminetetraacetic acid, and potassium hydroxide solutions, but could not be eluted using a thiourea–HCl solution. After the elution of Ir with a 6 M HCl solution, lyophilized cells could be reused up to five times for Ir recovery with over 60% efficiency. Scanning electron-assisted dielectric microscopy and scanning electron microscopy revealed that Ir accumulated in the cytosol of the lyophilized cells. X-ray absorption fine structure analysis demonstrated the formation of an outer–sphere complex between Ir and the cellular residues, suggesting the adsorption *via* ion exchange, and explaining the ability to elute the Ir and reuse the cells. Our results provide a scientific basis for inexpensive and environmentally friendly biosorbents as an alternative to ion-exchange resins for the recovery of Ir.

 Received 24th February 2023  
 Accepted 27th April 2023

DOI: 10.1039/d3ra01249b

[rsc.li/rsc-advances](https://rsc.li/rsc-advances)

## 1 Introduction

Iridium (Ir) is one of the rarest elements in Earth's crust.<sup>1</sup> Due to its high corrosion resistance, a trace amount of Ir is used in alloys in many industries for precision production of spark plugs, engine parts, and central processing unit boards, as well as homogeneous catalysts.<sup>1–4</sup> Only three tons of Ir are produced globally per year, mainly as a by-product of the electrolytic refining of copper and nickel,<sup>1</sup> and recycling is necessary from both economic and environmental standpoints.

To recycle trace amounts of Ir, electronic waste is dissolved with solutions containing Cl<sup>−</sup>, such as aqua regia.<sup>2,3,5–7</sup> Since the Ir(III) species is metastable to the Ir(IV) species, Ir(IV)Cl<sub>6</sub><sup>2−</sup> is commonly used as a comparatively stable chloride complex.<sup>5,8,9</sup> In general, a trace amount (10–50 mg L<sup>−1</sup>) of the precious metal is dissolved in polymetallic wastewater containing a large amount of Fe, Cu, and Ni.<sup>3,4,10–12</sup>

Chemical precipitation and adsorption *via* synthetic ion-exchange resin are often used to extract precious metals dissolved in chloride solutions;<sup>2,5</sup> however, they are suitable for large-scale recovery from medium to high-concentration solutions. In addition, Ir is often combined with rhodium (Rh) to make alloys and machinery; due to their similar chemical characteristics, separating Ir(IV) and Rh(III) is one of the most challenging processes in hydrometallurgy.<sup>2,5</sup> There is therefore still a need for an inexpensive and environmentally friendly Ir recovery method suitable for small-scale facilities or for recovering small amounts of Ir. In general, biosorbents (*e.g.*, living cells, dead biomass, and bio-industrial processes waste) are less expensive and have less environmental burden than recovery using synthetic ion-exchange resins.

*Galdieria sulphuraria* is a unicellular red alga belonging to the family Cyanidiophyceae.<sup>13</sup> Cyanidiophyceae is an extremophile that thrives in hot sulfur springs at a pH of less than five

<sup>a</sup>Faculty of Life and Environmental Sciences, University of Tsukuba, 1-1-1 Tennodai, Tsukuba, Ibaragi, 305-8572, Japan. E-mail: minoda.ayumi.gb@u.tsukuba.ac.jp; Fax: +81-29-853-6662; Tel: +81-29-853-6662

<sup>b</sup>School of Life and Environmental Sciences, University of Tsukuba, 1-1-1 Tennodai, Tsukuba, Ibaragi, 305-8572, Japan. E-mail: s1910551@s.tsukuba.ac.jp

<sup>c</sup>National Metrology Institute of Japan (NMIJ), National Institute of Advanced Industrial Science and Technology (AIST), 1-1-1 Umezono, Tsukuba, Ibaragi, 305-8563, Japan. E-mail: shinichi-miyashita@aist.go.jp

<sup>d</sup>Health and Medical Research Institute, National Institute of Advanced Industrial Science and Technology (AIST), Central 6, Higashi, Tsukuba, Ibaragi, 305-8566, Japan. E-mail: t-ogura@asit.go.jp

<sup>e</sup>Department of Earth and Planetary Science, the University of Tokyo, Hongo, Bunkyo-ku, Tokyo, 113-0033, Japan. E-mail: snatori@eps.s.u-tokyo.ac.jp; sunjing@eps.s.u-tokyo.ac.jp; ytakaha@eps.s.u-tokyo.ac.jp

† Electronic supplementary information (ESI) available. See DOI: <https://doi.org/10.1039/d3ra01249b>



and temperatures up to 56 °C. Among Cyanidiophyceae, only *Galdieria* has a metabolically flexible lifestyle, using over 27 types of sugar and polyols for their growth,<sup>14</sup> and is the most tolerant of various environmental stresses.<sup>13,15</sup> Thus, *Galdieria* spp. dominate the extreme conditions where it is difficult for other organisms to grow, representing up to 90% of the biomass in sulfur hot springs. These unique characteristics also make *Galdieria* spp. suitable for biotechnological uses, including the efficient production of biomass, biocrude oil, and beneficial compounds such as phycocyanin and floridosides,<sup>13,16–18</sup> as well as efficient wastewater treatment<sup>16,19</sup> and metal recovery.<sup>20–24</sup>

Our previous study comparing *G. sulphuraria* to the green alga *Chlorella vulgaris* has demonstrated the highly efficient recovery of Au and Pd from acidic solutions.<sup>21,25</sup> Furthermore, lyophilization of algal cells increased the recovery efficiencies of Au, Pd, and Pt from acidic solutions.<sup>23–26</sup> Here, we investigated the recovery of a trace amount of Ir from HCl solutions using lyophilized *G. sulphuraria* cells.

## 2 Materials and methods

### 2.1 Strain and culture conditions

Cells of *G. sulphuraria* 074W (NIES-3638) (500 mL) were grown in glass vessels with modified Allen's medium (pH 2.5) at 40 °C under continuous light (70  $\mu\text{E m}^{-2} \text{s}^{-1}$ ) following the methodology of Minoda *et al.* 2022.<sup>26</sup> The modified growth medium contained the following compounds ( $\text{g L}^{-1}$ ):  $(\text{NH}_4)_2\text{SO}_4$  (2.62);  $\text{KH}_2\text{PO}_4$  (0.54);  $\text{MgSO}_4 \cdot 7\text{H}_2\text{O}$  (0.5);  $\text{CaCl}_2 \cdot 2\text{H}_2\text{O}$  (0.14);  $\text{FeSO}_4 \cdot 7\text{H}_2\text{O}$  (0.016). In the medium, the concentrations of the trace elements were double of those in Arnon's A<sub>6</sub> solution,  $\text{H}_2\text{BO}_3$  was absent, and it contained the following compounds ( $\text{g L}^{-1}$ ):  $\text{MnCl}_2 \cdot 4\text{H}_2\text{O}$  (1.8);  $\text{ZnCl}_2$  (0.105);  $\text{Na}_2\text{MoO}_4 \cdot 2\text{H}_2\text{O}$  (0.39);  $\text{CoCl}_2 \cdot 6\text{H}_2\text{O}$  (0.04);  $\text{CuCl}_2$  (0.043). When the optical density at 750 nm had reached 2, the cells were collected and lyophilized (FZ-6SF; Labconco Corporation, Kansas City, MO, USA).

### 2.2 Sorption experiments

The lyophilized *G. sulphuraria* cells, activated carbon (Kuricoal WG160, Kurita, Japan), and a strongly basic anion-exchange resin (DIAION™ SA-10A, Mitsubishi Chemical, Japan) were used. The adsorbents (20 mg  $\text{mL}^{-1}$ ) were incubated in HCl solutions at 25 °C for 30 minutes, with a total reaction volume of 1 mL. Negative control reactions consisted of the same solutions with no added adsorbent. Ir was added as  $\text{H}_2\text{Ir(IV)Cl}_6$ , and all other metals were also added as chlorides.

The concentration of each metal in the adsorbent-containing supernatant was subtracted from its concentration in the negative control to obtain adsorbed metal concentration. Recovery efficiencies were determined by dividing the concentrations of adsorbed metals by their concentrations in the supernatant of the negative control. The supernatants were diluted 1000-fold with a solution containing 2.5 wt% HCl and 2.5 wt%  $\text{HNO}_3$ , and the concentrations of metals were determined by inductively coupled plasma mass spectrometry (Agilent 7700x ICP-MS, Agilent Technologies, USA).<sup>26</sup>

**Table 1** Desorption efficiencies of Ir from the Ir-adsorbed lyophilized *G. sulphuraria* cells

Desorption solution	Desorption efficiency (%)
6 M HCl	98 ± 7
0.5 M EDTA (pH 8)	93 ± 19
1 M thiourea/0.1M HCl	5.3 ± 0.8
1 M KOH	100 ± 5

### 2.3 Desorption experiment

Lyophilized cells were collected by centrifugation after incubation at 25 °C in a 0.2 M HCl solution containing 10 mg  $\text{L}^{-1}$  Ir for 30 minutes. The cells were washed once with water, then suspended in desorption solutions listed in Table 1 and allowed to incubate at 25 °C for 30 minutes. For desorption, they were incubated for 30 minutes. Desorption efficiencies were calculated by dividing the concentration of Ir in the supernatant obtained after desorption by the adsorbed Ir concentration in the lyophilized cells. The excess amount of Ir eluted when washed with water was less than 0.1 mg  $\text{L}^{-1}$ .

### 2.4 Scanning electron assisted dielectric microscopy (SE-ADM)

Lyophilized cells corresponding to 20 mg  $\text{mL}^{-1}$  were incubated for 30 minutes in a 0.2 M HCl solution with or without 1000 mg  $\text{L}^{-1}$  Ir. The Ir-adsorbed cells were washed twice with a 0.1 M HCl solution before the observation by electron microscopy. The observation was performed using a handmade SE-ADM imaging system, following the methodology of Okada and Ogura (2016).<sup>27</sup>

### 2.5 XAFS analysis

Lyophilized cells corresponding to 20 mg  $\text{mL}^{-1}$  were incubated for 30 minutes in a 0.2 M HCl solution with or without 10 mg  $\text{L}^{-1}$  Ir. Ir-adsorbed cells were filtered and washed once with a 0.2 M HCl solution. Ir L<sub>III</sub>-edge XAFS data were collected at beamline BL-9A at the Photon Factory (Tsukuba, Japan), following the methodology of Tanaka *et al.* (2017).<sup>28</sup> Fluorescence spectra were collected using a 7-element silicon drift detector (SDD). Data analyses were carried out using the code REX 2000 (Rigaku Co. Ltd, Japan).

## 3 Results and discussion

### 3.1 Ir recovery

**3.1.1 Ir recovery from HCl solutions.** First, we investigated Ir recovery from 0.1–1 M HCl solutions containing 10 mg  $\text{L}^{-1}$  Ir for 30 minutes of incubation. Ir was recovered in lyophilized *G. sulphuraria* cells with an efficiency of greater than 80% from acid concentrations up to 0.2 M acid, but the recovery efficiency decreased with increasing acid concentration, falling to 32% ± 5% in 1 M HCl (Fig. 1a). Recovery of 87% ± 0.4% of Ir from a 0.2 M HCl solution was achieved within 3 minutes, using 20 mg  $\text{mL}^{-1}$  lyophilized *G. sulphuraria* cells (Fig. S1†).



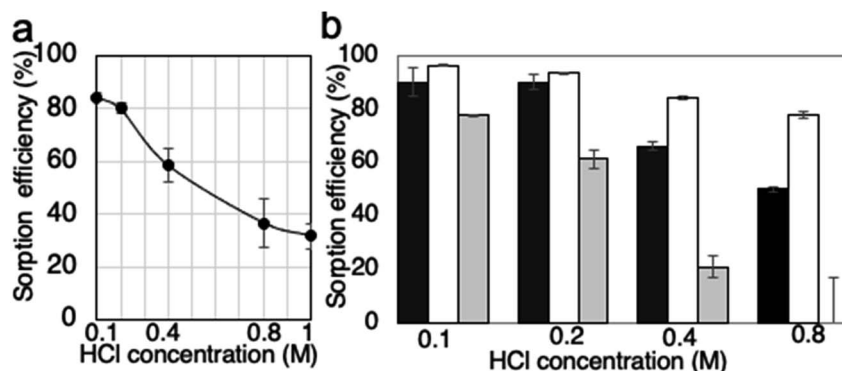


Fig. 1 (a) Sorption efficiency of Ir from 0.1–1 M HCl solutions containing 10 mg L<sup>-1</sup> Ir with lyophilized *Galdieria sulphuraria* cells. (b) Comparison of Ir sorption efficiencies from HCl solutions containing 10 mg L<sup>-1</sup> Ir. Lyophilized *G. sulphuraria* cells (black bar), an ion-exchange resin (white bar), and activated carbon (gray bar) were incubated in 0.1–0.8 M HCl solutions containing 10 mg L<sup>-1</sup> Ir. Values are the averages  $\pm$  SDs of three replicate assays.

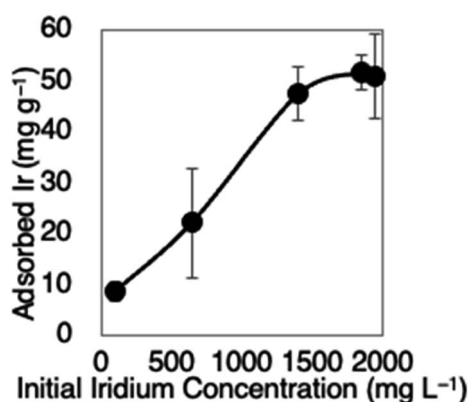


Fig. 2 Ir adsorbed from a 0.2 M HCl solution by lyophilized *G. sulphuraria* cells. Lyophilized *G. sulphuraria* cells were incubated in 0.2 M HCl solution containing Ir at the concentrations indicated in the figure. Values are the averages  $\pm$  SDs of three replicate assays.

The efficiency of Ir recovery was compared between lyophilized *G. sulphuraria* cells, a trimethyl ammonium-type ion-exchange resin, and activated carbon (Fig. 1b). The highest sorption efficiency was achieved by the ion-exchange resin, which recovered more than 78% of Ir at all acid concentrations.

However, lyophilized cells could recover Ir more efficiently than activated carbon at all acid concentrations, and at concentrations up to 0.2 M acid, the cells' sorption efficiency was comparable to that of the ion-exchange resin. The maximum sorption efficiency of Ir with activated carbon was 78%  $\pm$  0.2% at 0.1 M acid, which decreased to 0% at 0.8 M acid. Thus, lyophilized *G. sulphuraria* cells could recover small amounts of Ir more efficiently than activated carbon and work as well as an ion-exchange resin in less than 0.2 M HCl solutions.

**3.1.2 Adsorption capacity.** We determined the amount of Ir recovered from a 0.2 M HCl solution using lyophilized *G. sulphuraria* cells after 30 minutes of incubation (Fig. 2). The maximum amount of adsorbed Ir was 52  $\pm$  3.4 mg g<sup>-1</sup> at 1800 mg L<sup>-1</sup> Ir, which was comparable to the adsorption of the ion-exchange resin (47  $\pm$  5 mg g<sup>-1</sup>) in the same solution. However, the adsorption amounts were smaller than the maximum amounts obtained using ion-exchange resins containing thiosemicarbazide, piperazine, and tetrazine groups (410–430 mg g<sup>-1</sup>).<sup>7,29,30</sup> The lyophilized cells can be suitable for small-scale recovery of Ir from low-concentration solutions because their Ir adsorption capacity is smaller than that of ion-exchange resins designed for Ir adsorption.

**3.1.3 Selective recovery.** We tested the selective recovery of Ir from a poly-metallic solution containing 0.2 M HCl and

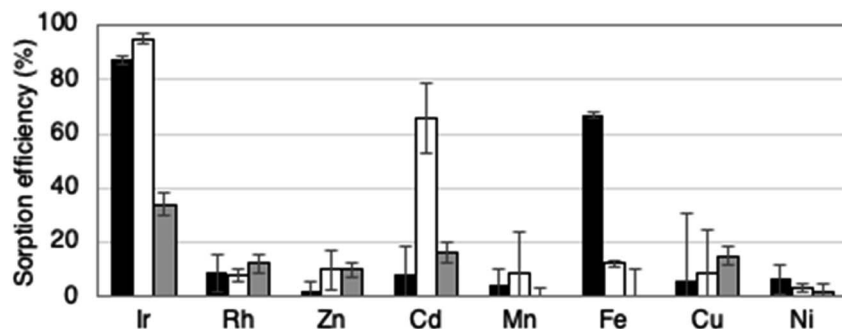


Fig. 3 Selective metal recovery from a 0.2 M HCl solution containing 20 mg L<sup>-1</sup> Ir, Rh, Zn, Cd, Mn, Fe, Cu, and Ni. Lyophilized *G. sulphuraria* cells (black bar), ion-exchange resin (white bar), and activated carbon (gray bar) were incubated in a 0.2 M HCl solution containing each metal. Values are the averages  $\pm$  SDs of three replicate assays.



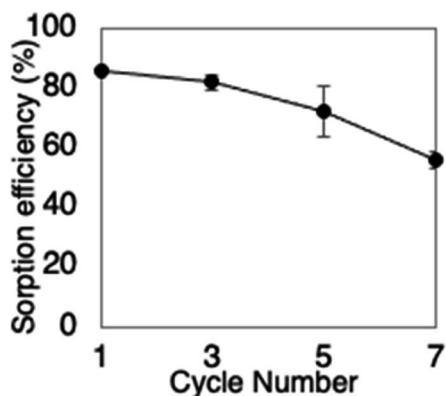


Fig. 4 Repeat adsorption of Ir in a 0.2 M HCl solution using lyophilized *G. sulphuraria* cells. Lyophilized *G. sulphuraria* cells were incubated in a 0.2 M HCl solution containing  $10 \text{ mg L}^{-1}$  Ir. After the elution of Ir using a 4 M HCl solution, the lyophilized cells were reused seven times to recover Ir. Values are the averages  $\pm$  SDs of three replicate assays.

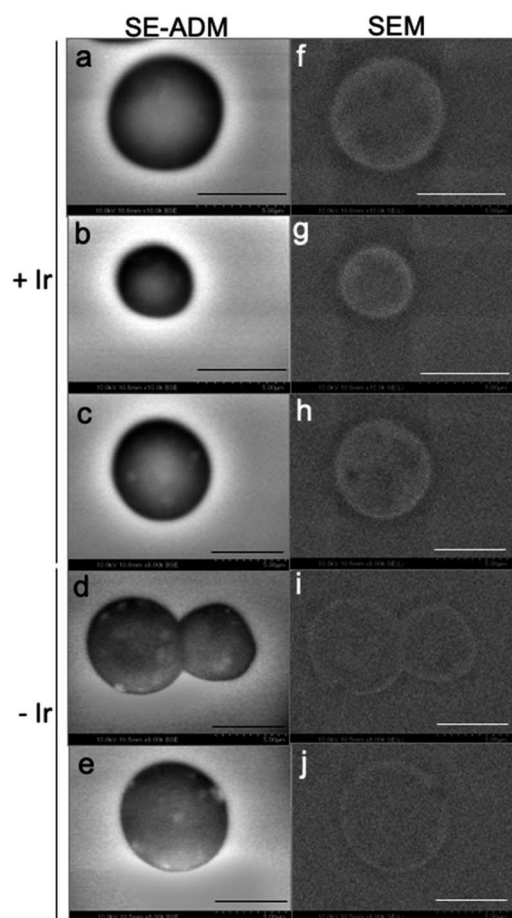


Fig. 5 Ir accumulates in the cytosol of the Ir-adsorbed lyophilized *G. sulphuraria* cells. Lyophilized cells were incubated in the presence (a–c, f–h) or absence (d, e, i and j) of  $1000 \text{ mg L}^{-1}$  Ir. (a–c) Dielectric images of a *G. sulphuraria* cells in the presence of Ir. (f–h) Simultaneously obtained SEM secondary electron images of (a–c). (d) and (e) Dielectric images of *G. sulphuraria* cells in the absence of Ir. (i) and (j) Simultaneous SEM secondary electron images of (d) and (e). Scale bar: 5  $\mu\text{m}$ .

$20 \text{ mg L}^{-1}$  each of Ir, Rh, Zn, Mn, Fe, Cu, and Ni using lyophilized *G. sulphuraria* cells, the ion-exchange resin, and activated carbon (Fig. 3). Lyophilized *G. sulphuraria* cells recovered Ir with  $83\% \pm 0.4\%$  efficiency and recovered Fe with  $91\% \pm 1.8\%$  efficiency. The ion-exchange resin recovered Ir with  $95\% \pm 0.1\%$  efficiency and recovered Cd with  $84\% \pm 0.2\%$  efficiency. The separating coefficients for Ir/Fe in lyophilized cells and the ion-exchange resin were 1.3 and 7.9, respectively, and for Ir/Cd were 11 and 1.4 (Table S1†). The efficiency of Ir recovery using activated carbon was  $34\% \pm 4\%$ , demonstrating that activated carbon is the least efficient Ir sorbent in a polymetallic solution as well.

Since very little Rh was recovered from HCl solutions using lyophilized cells (Fig. 3 and S1†), these cells could be useful for separating Ir from metal wastewater that also contains Rh. Conversely, the recovery of Fe in addition to Ir by lyophilized *G. sulphuraria* cells may be a disadvantage (Fig. 3). However, Ir alloys generally contain Rh, Cu, and Ni rather than Fe, rendering nonspecific adsorption of Fe less of an issue. In addition, a prior Fe removal step in metal waste processing could help to solve this problem.

**3.1.4 Desorption of adsorbed Ir.** We tested the desorption of the Ir adsorbed on the lyophilized cells (Table 1). The lyophilized cells with adsorbed Ir were incubated with the solutions listed in Table 1 for 30 minutes. The adsorbed Ir was eluted with over 90% efficiency in 6 M HCl, 0.5 M ethylenediaminetetraacetic acid (EDTA, pH 8), and 1 M potassium

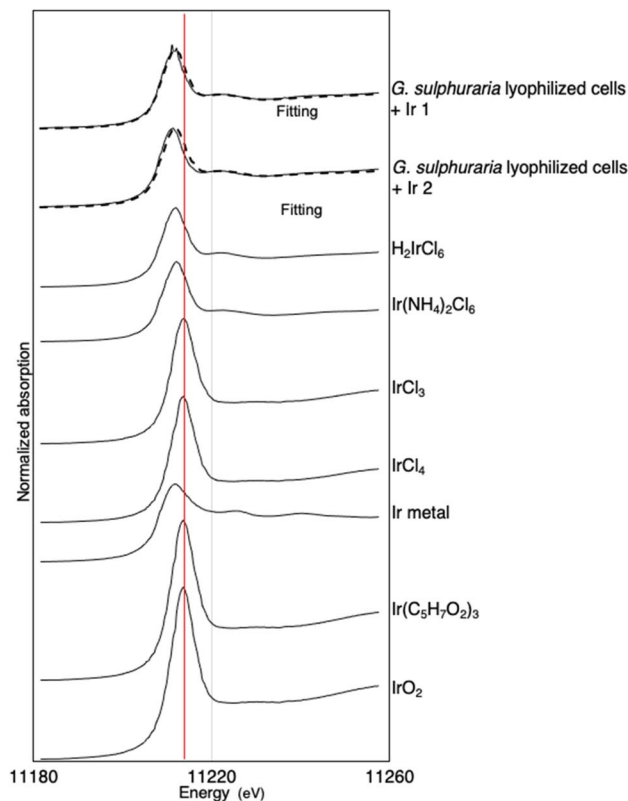


Fig. 6 Ir XANES spectra obtained from the Ir adsorbed on lyophilized *G. sulphuraria* cells and six reference materials. The dotted lines are fittings.



hydroxide (KOH) solutions, but was not eluted with incubation in 0.1 M HCl containing 1 M thiourea (Table 1). The Ir accumulated inside the lyophilized cells appeared to be chemically chelated to cellular residues, allowing the eluate to be used in chemical reactions during the subsequent purification process.

### 3.1.5 Reusability of *G. sulphuraria* cells for Ir adsorption.

Since Ir adsorbed in the lyophilized cells could be eluted in HCl solution, we tested the ability of the cells to be reused for subsequent adsorption (Fig. 4). The Ir-adsorbed cells were recovered and incubated with a 4 M HCl solution for 30 minutes to elute the Ir. After washing once with ionized water, the lyophilized cells were resuspended in a 0.2 M HCl solution containing 10 mg L<sup>-1</sup> Ir. The above procedure was repeated seven times to assess the cells' reusability. The lyophilized cells still recovered Ir from the solution with more than 80% efficiency after three repetitions, and 55% efficiency after seven (Fig. 4). The reversibility of Ir in lyophilized *G. sulphuraria* cells as Ir adsorbents is encouraging regarding their potential to reduce the recovery cost and environmental burden of industrial trace Ir recovery.

## 3.2 Mechanism of Ir recovery

**3.2.1 Localization of Ir.** To assess the accumulation of Ir in lyophilized *G. sulphuraria* cells, we conducted a SE-ADM analysis. Since SE-ADM allows direct observation of the sample

without pretreatment, the interaction between metals and cells is conserved during observation.<sup>27</sup> Regions in a darker color, with low electric permittivity, were more widespread in the lyophilized cells with adsorbed Ir than in the non-Ir-adsorbed cells (Fig. 5a–e). Similarly, the SEM electron beam reflection was stronger and more widespread in lyophilized cells with adsorbed Ir than in non-Ir-adsorbed cells (Fig. 5f–j). No electron beam reflections from microbody-like structures with high electric permittivity that accumulate metabolites such as lipids were observed (Fig. 5e and f). Ir is accumulated in the cytosolic spaces of the lyophilized cells.

**3.2.2 XAFS analysis.** To further elucidate the biosorption mechanism, we conducted an XAFS analysis (Fig. 6, 7, and S3†). X-ray absorption near-edge structure (XANES) provides information regarding the valence state and symmetry of metal complexes. In contrast, extended X-ray absorption fine structure (EXAFS) provides information on the interatomic distance to neighboring atoms and their coordination number. Simulation of EXAFS data can be used to provide direct metrical details of the metal–ligand environment.<sup>31</sup>

In the normalized XANES spectra (Fig. 6), the absorption edge, defined here as the energy when normalized absorption ( $\mu t$ ) is 0.5 ( $E_{\mu t=0.5}$ ), was 11 208 eV for the Ir adsorbed in lyophilized cells. The  $E_{\mu t=0.5}$  was the same for H<sub>2</sub>IrCl<sub>6</sub> and Ir(NH<sub>4</sub>)<sub>2</sub>Cl<sub>6</sub> (both also 11 208 eV). The edge energy was shifted by ~3 eV

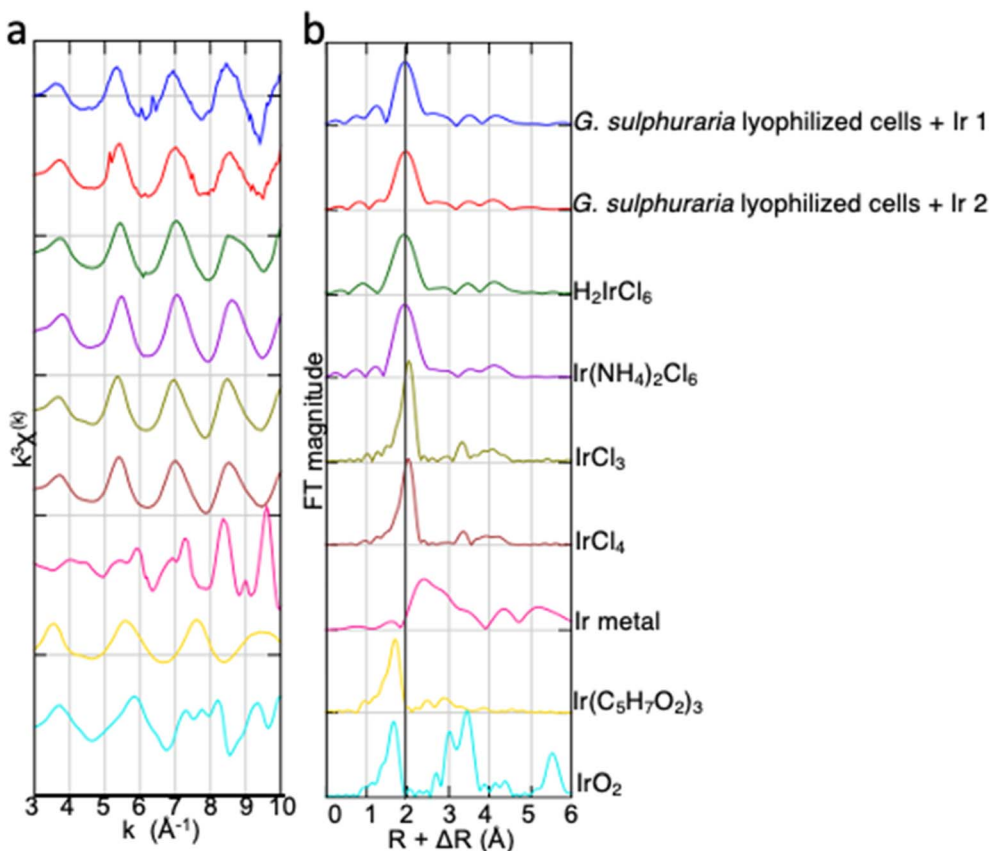


Fig. 7 EXAFS spectra of the Ir adsorbed on lyophilized *G. sulphuraria* cells and reference materials. (a)  $k^3$ -weighted  $\chi(k)$  EXAFS oscillations and (b) the corresponding RSFs.



relative to  $\text{IrCl}_3$ ,  $\text{IrCl}_4$ , and  $\text{IrO}_2$  (Fig. 6).<sup>32</sup> The linear combination (LC)-XANES fits for the Ir adsorbed on the cells also showed that the spectrum for this Ir was best matched to that of  $\text{Ir}(\text{IV})\text{-Cl}$  in  $\text{H}_2\text{IrCl}_6$  (Fig. S3†). The LC-XANES fitting of the cell-adsorbed Ir spectrum to  $\text{H}_2\text{IrCl}_6$  rather than  $\text{Ir}(\text{NH}_4)_2\text{Cl}_6$  may be due to the influence of a high concentration of Cl in the solution. These results suggest that Ir was adsorbed as  $\text{IrCl}_6^{2-}$  inside the lyophilized cells, possibly by forming an outer-sphere complex. The oscillation of the EXAFS function in  $k$ -space and the first peak in the radial structure functions (RSFs) of the Ir adsorbed on the cells was also successfully fitted by assuming the  $\text{Ir}(\text{IV})\text{-Cl}$  shell (Fig. 7). Thus, our results indicate that Ir is adsorbed on the cells by forming an outer-sphere complex, and therefore could be eluted *via* an ion-exchange reaction (Table 1).

**3.2.3 Ir adsorption *via* the formation of an outer-sphere complex.** A Langmuir model fitted with the experimental data suggested that single-site adsorption occurred (Table S2; Fig. S4†). Additionally, XANES and EXAFS spectra of the Ir adsorbed on the cells suggested the formation of an outer-sphere complex with Cl. The  $\text{IrCl}_6^{2-}$  complex forms an outer-sphere complex with  $\text{NH}_4^+$  and is known to be stable.<sup>33</sup> In lyophilized *G. sulphuraria* cells, most of the  $\text{IrCl}_6^{2-}$  can likely form an outer-sphere complex with amine groups derived from proteins or other cellular compounds in the cytosol (Table 1; Fig. 5–7). This is also consistent with the higher recovery efficiency of Ir (present as  $\text{Ir}^{4+}$  in this study) than of Rh ( $\text{Rh}^{3+}$ ) by lyophilized cells, and the fact that this was similar in the anion-exchange resin but opposite in the cation-exchange resin (Fig. 3 and S1†).<sup>34</sup> The difference in metal selectivity between lyophilized cells and ion-exchange resin may be due to the difference between the amine groups present in the lyophilized cells and the trimethylammonium groups in the ion-exchange resin (Fig. 3).

The higher efficiency of Ir recovery from HCl solutions by using lyophilized *G. sulphuraria* cells than by using activated carbon (Fig. 1b and 3) may be due to the difference between lyophilization and heat treatment. In general, lyophilized biomaterial retains the variation in cellular residues better than activated carbon made by heat treatment.<sup>24,35–37</sup> Understanding the details of this adsorption mechanism and the similarities and differences between these cells and other adsorbents will be an area of future study necessary to accelerate the development of high-performance Ir biosorbents.

## 4 Conclusion

Here, we showed that lyophilized *G. sulphuraria* cells could recover low concentrations of Ir from HCl solutions with high efficiency and selectivity. The Ir accumulated in the cytosol of the cells and formed an outer-sphere complex with cellular residues. The recovery efficiency of Ir from solutions containing up to 0.2 M acid using *G. sulphuraria* was similar to that obtained using an ion-exchange resin, and overall higher than recovery efficiency with activated carbon. The selectivity for other metals differed between *G. sulphuraria* cells and the ion-exchange resin, indicating that the two methods might be useful in different waste adsorption scenarios. Since this Ir

recovery was based on ion-exchange, the Ir can be eluted and the cells reused. We found that the cells could be reused five times to recover Ir from a 0.2 M HCl solution, retaining over 60% efficiency. These results suggest that lyophilized biomaterials such as *G. sulphuraria* can be useful as an alternative to ion-exchange resins for the recovery of trace amounts of Ir.

## Abbreviations

ICP-MS	Inductively coupled plasma-mass spectrometry
SE-ADM	Scanning electron assisted dielectric microscopy
SEM	Scanning electron microscopy
XAFS	X-ray absorption fine structure
XANES	X-ray absorption near-edge structure
EXAFS	Extended X-ray absorption fine structure

## Author contributions

A. M., S. U., S. M., T. O., S. N, J. S., and Y. T. investigation; A. M., and T. O. visualization; A. M. writing-original draft; S. U., S. M., T. O., S. N, J. S., and Y. T. writing-review & editing; A. M. funding acquisition and conceptualization.

## Conflicts of interest

The authors declare that they have no known competing financial interests or personal relationships that could have appeared to influence the work reported in this paper.

## Acknowledgements

This work was supported by Grant-in-Aid for Scientific Research (C) (18K05922) and Nakatsuji Foresight Foundation Research Grant to A. M. XAFS analysis was conducted with the approval of KEK-PF (2020G081). A part of the XAFS spectrum for the reference sample of Ir is utilized by SPring-8 BL14B2 XAFS database. We would like to thank Gene Research Center, the University of Tsukuba.

## References

- 1 D. Payne, *Nat. Chem.*, 2016, **8**, 392.
- 2 P. P. Sun and M. S. Lee, *Hydrometallurgy*, 2011, **105**, 334–340.
- 3 Y. Chen, M. Xu, J. Wen, Y. Wan, Q. Zhao, X. Cao, Y. Ding, Z. L. Wang, H. Li and Z. Bian, *Nat. Sustain.*, 2021, **4**, 618–626.
- 4 C. A. Kohl and L. P. Gomes, *J. Clean. Prod.*, 2018, **184**, 1041–1051.
- 5 C. S. Kedari, M. T. Coll, A. Fortuny, E. Goralska and A. M. Sastre, *Hydrometallurgy*, 2006, **82**, 40–47.
- 6 M. Knothe, K. Schwarz and H. Förster, *J. Less-Common Met.*, 1991, **168**, 249–255.
- 7 Y.-Y. Chen, C. Liang and Y. Chao, *React. Funct. Polym.*, 1998, **36**, 51–58.
- 8 N. N. Greenwood and A. Earnshaw, *Chemistry of the Elements*, Elsevier, 2012.



- 9 D. G. Brookins, *Eh-pH Diagrams for Geochemistry*, Springer, Berlin, Heidelberg, 1988.
- 10 L. Zhang and Z. Xu, *J. Clean. Prod.*, 2016, **127**, 19–36.
- 11 H. Umeda, A. Sasaki, K. Takahashi, K. Haga, Y. Takasaki and A. Shibayama, *Mater. Trans.*, 2011, **52**, 1462–1470.
- 12 G. Petrov, I. Zotova, T. Nikitina and S. Fokina, *Metals*, 2021, **11**, 569.
- 13 J. Van Etten, C. H. Cho, H. S. Yoon and D. Bhattacharya, *Semin. Cell Dev. Biol.*, 2023, **134**, 4–13.
- 14 W. Gross and C. Schnarrenberger, *Plant Cell Physiol.*, 1995, **36**, 633–638.
- 15 G. Schönknecht, W.-H. Chen, C. M. Ternes, G. G. Barbier, R. P. Shrestha, M. Stanke, A. Bräutigam, B. J. Baker, J. F. Banfield, R. Michael Garavito, K. Carr, C. Wilkerson, S. A. Rensing, D. Gagneul, N. E. Dickenson, C. Oesterhelt, M. J. Lercher and A. P. M. Weber, *Science*, 2013, **339**, 1207–1210.
- 16 K. P. R. Dandamudi, M. Mathew, T. Selvaratnam, T. Muppaneni, M. Seger, P. Lammers and S. Deng, *Resour. Conserv. Recycl.*, 2021, **171**, 105644.
- 17 O. S. Graverholt and N. T. Eriksen, *Appl. Microbiol. Biotechnol.*, 2007, **77**, 69–75.
- 18 T. Sakurai, M. Aoki, X. Ju, T. Ueda, Y. Nakamura, S. Fujiwara, T. Umemura, M. Tsuzuki and A. Minoda, *Bioresour. Technol.*, 2016, **200**, 861–866.
- 19 F. Abiusi, E. Trompetter, A. Pollio, R. H. Wijffels and M. Janssen, *Front. Microbiol.*, 2022, **13**, 820907.
- 20 A. Minoda, H. Sawada, S. Suzuki, S.-I. Miyashita, K. Inagaki, T. Yamamoto and M. Tsuzuki, *Appl. Microbiol. Biotechnol.*, 2015, **99**, 1513–1519.
- 21 X. Ju, K. Igarashi, S.-I. Miyashita, H. Mitsunashi, K. Inagaki, S.-I. Fujii, H. Sawada, T. Kuwabara and A. Minoda, *Bioresour. Technol.*, 2016, **211**, 759–764.
- 22 Y.-L. Cho, Y.-C. Lee, L.-C. Hsu, C.-C. Wang, P.-C. Chen, S.-L. Liu, H.-Y. Teah, Y.-T. Liu and Y.-M. Tzou, *Chem. Eng. J.*, 2020, **401**, 125828.
- 23 S.-I. Miyashita, T. Ogura, S.-I. Fujii, K. Inagaki, Y. Takahashi and A. Minoda, *J. Hazard. Mater. Adv.*, 2021, **3**, 100015.
- 24 S.-I. Miyashita, T. Ogura, T. Kondo, S.-I. Fujii, K. Inagaki, Y. Takahashi and A. Minoda, *J. Hazard. Mater.*, 2022, **425**, 127982.
- 25 A. Minoda, S.-I. Miyashita, T. Kondo, T. Ogura, J. Sun and Y. Takahashi, *RCR Advances*, 2023, **17**, 200140.
- 26 A. Minoda, S.-I. Miyashita, S.-I. Fujii, K. Inagaki and Y. Takahashi, *J. Hazard. Mater.*, 2022, **432**, 128576.
- 27 T. Ogura, *Biochem. Biophys. Res. Commun.*, 2015, **459**, 521–528.
- 28 K. Tanaka, M. Tanaka, N. Watanabe, K. Tokunaga and Y. Takahashi, *Chem. Geol.*, 2017, **460**, 130–137.
- 29 Z. Hubicki, M. Wawrzekiewicz, G. Wójcik, D. Kołodyńska and A. Wołowicz, in *Ion Exchange*, ed. A. Kilislioglu, IntechOpen, Rijeka, 2015.
- 30 C. Yi-Yong and Y. Xing-Zhong, *React. Polym.*, 1994, **23**, 165–172.
- 31 J. E. Penner-Hahn, *Elsevier Oceanogr. Ser.*, 2005, **eLS**, 174.
- 32 Z. Zhang, C. Feng, C. Liu, M. Zuo, L. Qin, X. Yan, Y. Xing, H. Li, R. Si, S. Zhou and J. Zeng, *Nat. Commun.*, 2020, **11**, 1215.
- 33 H. Renner, G. Schlamp, I. Kleinwächter, E. Drost, H. M. Lüscho, P. Tews, P. Panster, M. Diehl, J. Lang, T. Kreuzer, A. Knödler, K. A. Starz, K. Dermann, J. Rothaut, R. Drieselmann, C. Peter, R. Schiele, J. Coombes, M. Hosford and D. F. Lupton, *Ullmann's Encycl. Ind. Chem.*, 2018, 1–73.
- 34 A. G. Marks and F. E. Beamish, *Anal. Chem.*, 1958, **30**, 1464–1466.
- 35 H. Niu and B. Volesky, *J. Chem. Technol. Biotechnol.*, 2001, **76**, 291–297.
- 36 V. Tigrini, V. Prigione, I. Donelli, A. Anastasi, G. Freddi, P. Giansanti, A. Mangiavillano and G. C. Varese, *Appl. Microbiol. Biotechnol.*, 2011, **90**, 343–352.
- 37 M. Wojnicki, M. Luty-Blocho, R. P. Socha, K. Mech, Z. Pędzich, K. Fitzner and E. Rudnik, *J. Ind. Eng. Chem.*, 2015, **29**, 289–297.

